Study of Deposition Offset in Plasma Spray of Zirconia

W.H. Zhuang[1], D. Gray[2], K. Etemadi[3], and D.M. Benenson[3]

1. SUNY at Buffalo, Department of Mechanical and Aerospace Engineering, Buffalo, NY 14260
2. General Electric Corporation, Research and Develop Center, Schenectady, NY 12301
3. SUNY at Buffalo, Department of Electrical and Computer Engineering, Buffalo, NY 14260

Numerical modeling and experimental measurements have been performed to study the effects of powder carrier gas flow rates and powder sizes on the deposition offset in a plasma spray of yttria-stablized zirconia. The mathematical model involved simultaneous solution of the continuity, momentum and energy equations of the plasma gas, the dynamics and heat transfer of powder particles in the plasma, and the coupling effects between the plasma and particles. Experiments included measurement of particle velocities by laser strobe technique and measurement of deposition offset. Calculated plasma temperatures and velocities are greater than 13,000 K and 2,000 m/s, respectively, in the vicinity of nozzle exit. For the plasma-particle momentum transfer, the drag coefficient was computed in two ways- with corrections accounting for the strongly varying plasma properties, and without these corrections. Calculated and experimental results, in respect to deposition offset, are in agreement to within 25% when calculated without varying properties corrections, and within about 40% with corrections; agreement in respect to average particle velocities is within 20% when calculated without varying properties corrections, and within the range 30-50% with corrections.

INTRODUCTION

Applications of plasma sprayed coatings address wear resistance, temperature and oxidation resistance, corrosion resistance, etc. The present paper studies yttria-stablized zirconia coatings, which are widely used for the thermal protection of high-temperature components in gas turbine and diesel engines. In advanced engines, ceramic coatings also have to serve as both thermal and chemical barriers.

In spite of the development of plasma spray techniques in recent years, improved fundamental knowledge of the plasma dynamics, plasma-particle interactions, and coating dynamics is necessary for improving process control. Since many operational parameters control the spraying process, effective numerical models may help to optimize these parameters. In this paper, we study the plasma dynamics, particle dynamics and heat transfer, and their interactions. The measurements of deposition offsets and particle velocities provide a guide to better understand the particle dynamics and heat transfer model.

Mathematical modeling of flow, temperature and turbulence of the plasma plume has obtained increasing attention over the last several years. Earlier work used the boundary-layer (parabolic) approach to represent the plasma plume[1-3]. This method may not fully address the flow in the plasma spray process, in which a substrate is presented and the flow is no longer parabolic, especially near the substrate. In [4], the plasma jet with side-stream injection was modeled utilizing an elliptic model.

In the present paper, the elliptic model is used.

EXPERIMENTAL SETUP

A Metco torch, model 9MB with a G anode and 63 cathode were used in all experiments and modeling. Torch operating parameters were: current 500 A, voltage 73 V, torch efficiency 59.2%, primary gas (N_2) 80 scfh, secondary gas (H_2) 15 scfh. A spray dried and sintered 8% Yttria stablized zirconia powder, made by Starck, having average sizes of 25, 40, 53, 68, and 90 μm, with carrier gas (N_2) flow rates of 8, 11, 14, and 17 scfh, were studied. Powder feeding rate was 3 lb/hr. Particles were injected 5 mm downstream from the nozzle exit.

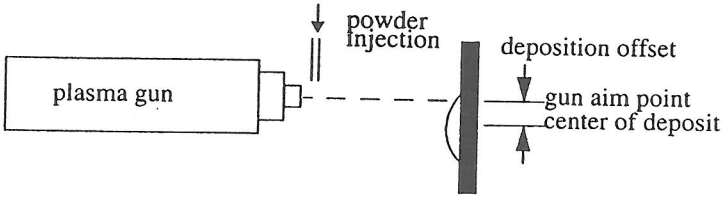

Fig.1. Schematic of the plasma spray system.

An Asea 2000 robot was used for the plasma gun manipulation. Deposits were applied to 4″ square 1/8″ thick metal plates. Precise measurements of the plasma gun aim point on the metal plates were made before coating. Location of the gun aim point on the plates were made by using a pointer machined to fit in the nozzle of the gun. The gun aim point was then referenced from machined edges of the metal substrate. The robot was used to articulate the plasma gun perpendicular to the direction of the powder injection to create a stripe of deposit. Multiple passes of the gun were made during the deposition process in order to built up enough material (≈0.010″) to accurately locate the thickest area of the deposit. The deposition offset was found by substracting the difference between the gun aim point and the location of the thickest point of the deposit. An illustration of how deposit offset was determined is shown in Fig. 1. Location of the thickest area of the deposit was also confirmed by cross sectioning the deposit and doing metallography.

Particle velocity measurements were taken using a Control Vision Laser strobe. Measurements were taken at the exit of the injector and at the location of the substrate for each powder size and powder carrier gas flow combination. Multiple measurements were taken for each condition and then averaged.

NUMERICAL MODELS

Numerical modeling first solved the conservation equations of mass, momentum, and energy of the plasma gas. Turbulent effects were represented by the k-ε model. The calculated flow and temperature fields were used to solve the particle dynamics and heat transfer in the plasma. Coupling effects between plasma and particles were then considered. Thermodynamic and transport properties of the plasma gas mixture were calculated. The mixture components considered in the calculation are: N_2, N_2^+, N, N^+, N^{2+}, H_2, H, H^+, e.

Particle dynamics and heat transfer in plasma may be affected by the following mechanisms: (1)strongly varying plasma property effects on viscous drag and convective heat transfer; (2) non-continuum effects; (3) turbulent dispersion; (4) particle shape; (5) evaporation; (6)heat conduction inside the particle; and (7) electric charging of particles. In the present paper, effects (1), (2), and (3) are considered in particle dynamics and heat transfer. The particle shape effect (4) was included in the drag force calculation. The evaporation effect (5) was considered in particle heat transfer. The electric charge effect (7) has little influence on particle movement and heat transfer

under continuum conditions (particle size > 10μm), and was neglected in our calculation. Although Bi number reached 0.1 during the particle movement in plasma, the internal heat conduction (6) was neglected for simplicity.

Due to the small size(25-90μm) of particles used, the drag force exerted on particles was treated as in the creeping flow problem. A simple form of drag coefficient has been adopted

$$C_D = \frac{24}{Re} + \frac{6}{1+\sqrt{Re}} + 0.4 \qquad (4)$$

where the properties for calculating Re are based on the film temperature, which is the average of the particle temperature, T_w, and the plasma temperature, T_∞.

There are several models for modifying the drag coefficient[4-6] and the heat transfer coefficient[4,5,7-9]. For purposes of comparison, the drag coefficient was calculated in two ways, i.e., with correction due to varying plasma properties, as suggested by Lee[5], and without this correction. In both the above cases, we have adopted the modification that considers the non-continuum effect (Chen[6]) and the correction of heat transfer coefficient due to varying plasma properties (Fiszdon[7]).

RESULTS AND DISCUSSION

Particle injection velocities were measured by the laser strobe technique (Fig. 2) and utilized as the initial conditions in modeling.

Figures 3-5 show the calculated plasma temperature, velocity and N2-H2 concentration, respectively. The temperature and velocity are higher than 13,000 K and

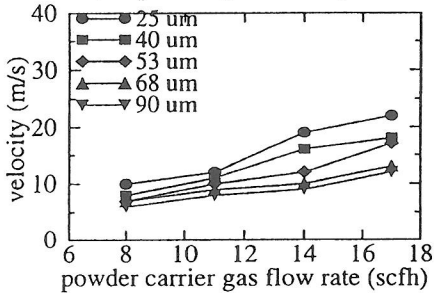

Fig. 2. Measured particle injection velocity.

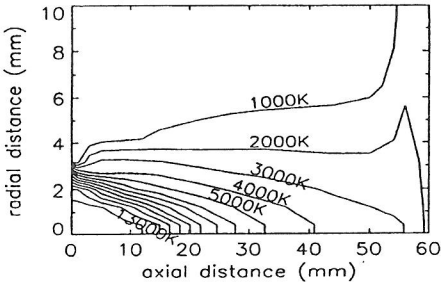

Fig. 3. Plasma temperature distribution (500A, 80scfh N_2, 15scfh H_2).

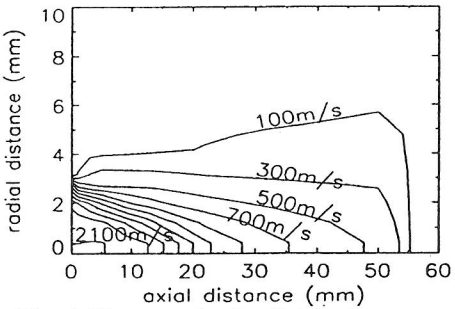

Fig. 4. Plasma velocity distribution (500A, 80scfh N_2, 15scfh H_2).

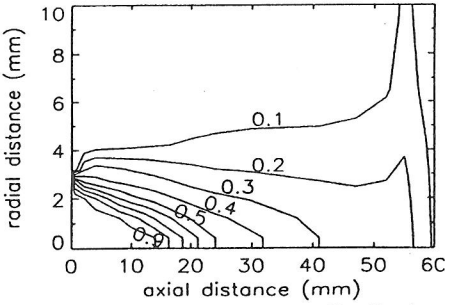

Fig. 5. N_2-H_2 concentration distribution (500A, 80scfh N_2, 15scfh H_2).

2,000 m/s, respectively, in the vicinity of nozzle exit. However, the entrained environmental air cools the plasma plume rapidly as axial distance increases. At 42mm from nozzle exit, the plasma temperatures are less than 4,000 K, as shown in Figure 3. This entrainment effect is illustrated clearly via the N2-H2 concentration contours shown in Figure 5. At a distance of 42 mm, the plume contains about 70% air in volume. Air is a mixture of molecules dissociated at relatively low temperature. The dissociation process absorbs a large amount of energy from the plume, and cools it efficiently. The shape changes of the temperature and concentration contours near axial distance of 57 mm are the results of substrate.

Figure 6 illustrates the measured deposition offsets. Figures 7 and 8 show the calculated deposition offsets, without and with varying properties corrections, respectively. The deposition offset is defined as the location of maximum mass accumulation off the axis of plasma torch. It is believed that the varying plasma properties effect plays an important role in particle movement in the thermal plasma. In our calculations, however, the deposition offsets predicted without the varying properties correction on drag coefficients are always closer to measured values (Fig. 9). That the measured offsets are larger than those calculated suggests that the drag forces exerted on particles were overestimated. The drag coefficients calculated with corrections [5] are greater than those without corrections. Particles with greater drag forces tend to stay in the plasma core region (high temperature and velocity region) longer and yield smaller deposition offsets. Except for the 25 μm particles, agreement between the measured and calculated offsets is within 25% for the case without varying properties corrections, and within about 40% for those with corrections.

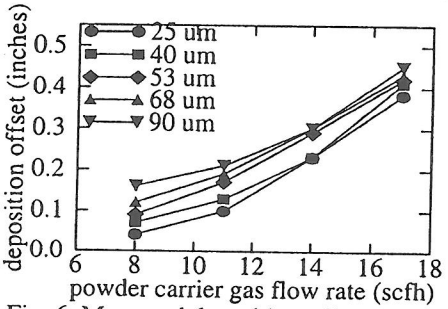

Fig. 6. Measured deposition offset (500A, 80scfh N_2, 15scfh H_2).

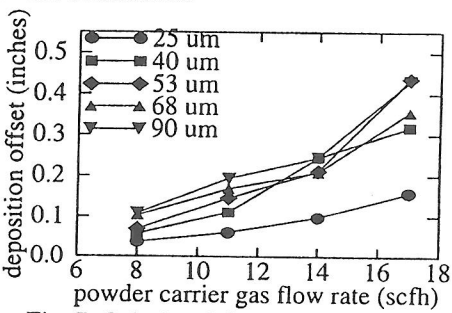

Fig. 7. Calculated deposition offset without varying properties correction (500A,80scfh N_2, 15scfh H_2).

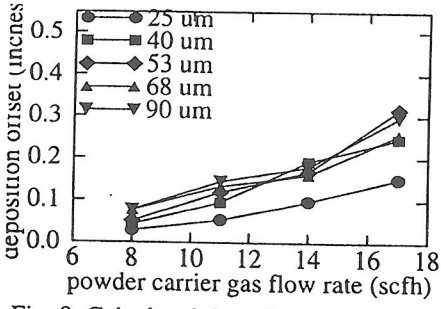

Fig. 8. Calculated deposition offset with varying properties correction (500A,80scfh N_2, 15scfh H_2).

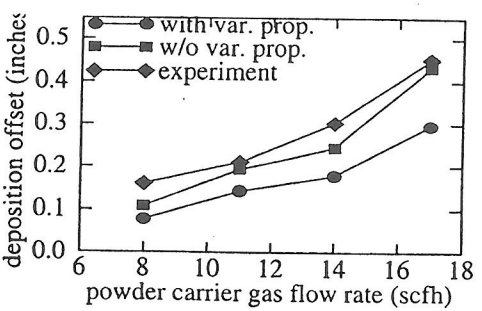

Fig. 9. Comparisons of deposition offset (500A, 80scfh N_2, 15scfh H_2, D=90 μm).

Figure 10 shows the measured average particle velocities at the offset. Figures 11 and 12, respectively, present the average velocities calculated without and with the varying properties corrections on drag coefficient. Similar to the deposition offsets, the particle velocities calculated without varying property corrections are closer to those measured (Fig. 13). As mentioned above, particles stayed in plasma core region longer when the drag coefficients were calculated with corrections; therefore, for this case, particles reached higher velocities through momentum transfer with the plasma gas. Particle velocities obtained by modeling agreed with those obtained from experiment to within 20%, except for 25 μm and 40 μm diameter particles having carrier gas flow rates of 8, and 11scfh, without the varying property corrections. Differences in the range 30%-50% were found for the case with corrections. Modeling failed to predict reasonable velocities and deposition offsets for the 25μm diameter particles due to their partial or total evaporation. Total evaporation, however, did not take place in the experiment. This result indicates that the particle temperatures were overpredicted, which is associated with neglect of the cooling effect of the carrier gas on plasma flow and temperature.

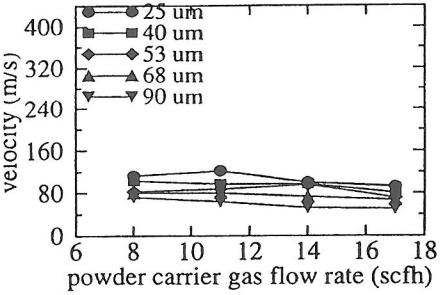

Fig. 10. Measured average particle velocities at offset (500A, 80scfh N_2, 15scfh H_2).

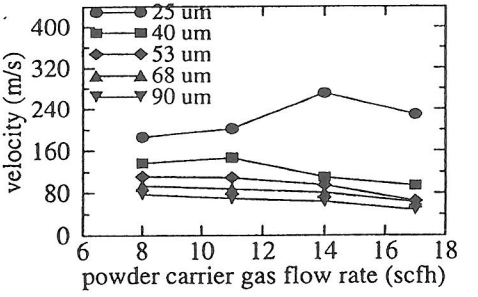

Fig. 11. Calculated particle velocities at offset without varying properties correction (500A, 80scfh N_2, 15scfh H_2).

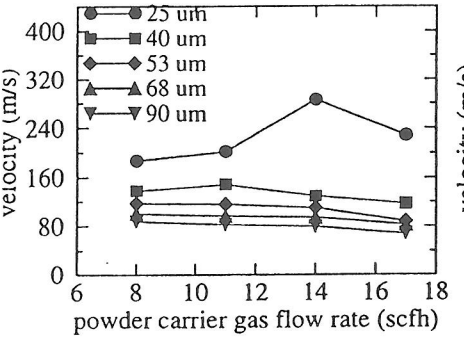

Fig. 12. Calculated particle velocities at offset with varying properties correction (500A, 80scfh N2, 15scfh H_2).

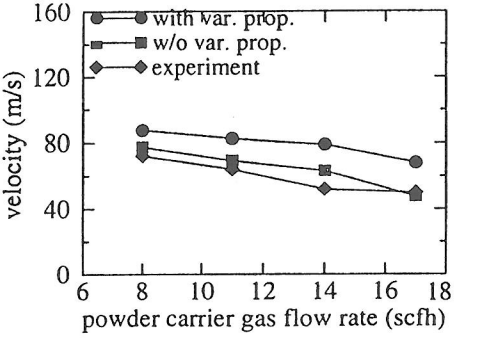

Fig. 13. Comparisons of particle velocities (500A, 80scfh N_2, 15scfh H_2, D=90 μm).

SUMMARY

This numerical and experimental study investigated plasma gas dynamics, particle dynamics and heat transfer in plasma spray processes. The plasma dynamics calculation illustrates that large amounts of entrained air lower the particle temperature considerably. Yttria-stablized zirconia powder with average sizes of 25, 40, 53, 68 and 90μm diameter, and carrier gas flow rates of 8, 11,14 and 17 scfh, were used. Deposition offsets and average particle velocities at the offset were measured and computed. The offsets and velocities calculated without the varying property corrections were closer to those measured than those with corrections. The drag coefficient calculated with corrections were overestimated, which caused the particles to stay in the plasma core region longer and thereby, yielded smaller offsets and larger velocities at offset. Agreement in deposition offsets, between modeling and experiment, was within 25% when calculated without varying properties effect corrections, and within 40% with corrections. The calculated average particle velocities agreed with those measured to within 20% when computed without varying properties corrections, and to within 30-50% with corrections. For the 25μm diameter particles, the relatively poor agreement between modeling and experiment results is associated with particle evaporation prior to impact on the substrate.

REFERENCES

1. Y. C. Lee, "Modeling work in thermal plasma processing", Ph.D Thesis, University of Minnesota, 1984.
2. J. Varacalle, Jr. R. L. Miller, J. A. Walter, and G. Irons, "Analytically Modeling The Plasma Spraying of Nickle-Aluminum Powder", ASME, HTD-Vol. 161, Heat Transfer in Thermal Plasma Processing, pp. 137-143, 1991.
3. A. H. Dilawari, J. Szekely, F. Coudert, and P. Fauchais, "Fluid Flow and Heat Transfer in Plasma Reactors- II. A Critical Comparison of Experimentally Measured and Theoretically Predicted Temperature Profiles in Plasma Jets in the Absence and Presence of Side-stream Injection", Int. J. Heat Transfer, Vol. 32, pp. 35-46, 1989.
4. J.A. Lewis, and W.H. Gauvin, "Motion of Particle Entrained in a Plasma Jet", AIChE J. Vol. 19, pp. 982-990, 1973.
5. Y. C. Lee, K. C. Hsu, and E. Pfender, "Modeling of Particles Injected into a D. C. Plasma Jet", 5th Inter. Symp. Plasma Chem., Vol. 2, pp. 795-803, 1981:Heriot-Watt Univ., Edingburgh, Scotland.
6. X. Chen, and E. Pfender, "Effect of the Knudsen Number on Heat Transfer to a Particle Immersed into a Thermal Plasma", Plasma Chemistry and Plasma Processing, Vol. 3, pp. 97-113, 1983.
7. J. K. Fiszdon, "Melting of Powder Grains in a Plasma Flame", Int. J. Heat Mass Transfer, Vol. 22, pp. 749-761, 1979.
8. N. N. Sayegh, and W.H. Gauvin, "Numerical Analysis of Variable Properties Heat Transfer to a Single Sphere in High Temperature Surroundings", AIChE J., Vol. 25, pp. 522-534, 1979.
9. M. Vardelle, A.Vardelle, P. Fauchais, and M. I. Boulos, "Plasma-Particle Momentum and Heat Transfer: Modeling and Measurement", AIChE J., Vol. 29, pp. 236-243, 1983.